VOL. 18, NO. 4, FEBRUARY 2023 ISSN 1819-6608
ARPN Journal of Engineering and Applied Sciences
©2006-2023 Asian Research Publishing Network (ARPN). All rights reserved.
www.arpnjournals.com

MAXWELL-NANOFLUID FLOW, HEAT AND MASS TRANSFER PAST A STRETCHING SHEET WITH MULTIPLE SLIP, HEAT SOURCE AND CHEMICAL REACTION EFFECTS USING FEM

Khaja Hassan[1], R. Vijaya Kumar[2] and G. Srinivas[1]
[1]Department of Mathematics, Guru Nanak Institute of Technology, Khanapur, Ibrahimpatnam, Hyderabad, Telangana State, India
[2]Mathematics Section, Faculty of Engineering and Technology, Annamalai University, Annamalainagar, Chidambaram, Tamilnadu, India
E-Mail: khaja.h4u@gmail.com

ABSTRACT

The research of chemical reactions besides three unique slip scenarios (velocity, thermal, and solutal) past a stretching sheet is of greater importance in convective heat and mass transfer studies. The Maxwell nano-fluid consists of nano-sized metal particles. Modeling it using coupled non-linear partial differential equations is one of the fascinating study issues. Partial differential equations describe the processes of fluid motion, temperature, and mass transfer. The corresponding boundary conditions are the Neumann boundary conditions. The solution of these partial differential equations subject to the Neumann boundary conditions necessitates a numerical investigation. The Finite Element method is adopted to simulate the results. The profiles of velocity, temperature, and diffusion are described for various non-dimensional parameters. The rates of heat transmission, mass and heat transfer, and skin friction are tabulated and described. The results are confirmed by comparison with existing literature and found to be in good agreement.

Keywords: maxwell fluid, nanofluid, stretching sheet; multiple slip, chemical reaction, finite element method.

Nomenclature:

List of Symbols

u, v : Velocity components in x and y axes respectively (m/s)
x, y : Cartesian coordinates measured along the stretching sheet (m)
f : Dimensionless stream function
f' : Fluid velocity (m/s)
Pr : Prandtl number
Du : Modified Dufour parameter
Sr : Dufour solutal Lewis number
C : Fluid concentration $\left(mol/m^3\right)$
B_o : Uniform magnetic field
C_∞ : Dimensional ambient volume fraction $\left(mol/m^3\right)$
T : Fluid temperature $\left(K\right)$
T_w : Temperature at the surface $\left(K\right)$
T_∞ : Temperature of the fluid far away from the stretching sheet $\left(K\right)$
O : Origin
M : Magnetic field parameter
Ln : Nanofluid Lewis number
L_1 : Slip length (m)
C_w : Dimensional concentration at the stretching surface $\left(mol/m^3\right)$
Cf : Skin-friction coefficient
Nur : Reduced rate of heat transfer coefficient (or) Reduced Nusselt number
Sh : Rate of mass transfer coefficient (or) Sherwood number
Shr : Reduced rate of mass transfer coefficient (or) Reduced Sherwood number
C_f : Specific heat capacity at constant pressure
C_p : Specific heat capacity of nano particle material
U : Reference velocity $\left(m/s\right)$
Le : Lewis number
Nb : Brownian Motion parameter
Nt : Thermophoresis parameter
D_B : Brownian diffusion coefficient
D_T : Thermophoresis diffusion coefficient
D_{CT} : Soret diffusivity
D_{TC} : Dufour diffusivity
D_S : Solutal diffusivity
a : Positive real number
S : Concentration profiles $\left(mol/m^3\right)$
L_2 : Thermal slip length (m)
K : Chemical reaction parameter
L_3 : Concentration slip length (m)

Greek Symbols

η : Dimensionless similarity variable
θ : Dimensionless temperature $\left(K\right)$

©2006-2023 Asian Research Publishing Network (ARPN). All rights reserved.

φ : Nanofluid Fluid concentration $\left(mol/m^3\right)$

φ_∞ : Dimensional Nanofluid volume fraction $\left(mol/m^3\right)$

φ_w : Dimensional Nanofluid concentration at the stretching surface $\left(mol/m^3\right)$

ϕ : Dimensionless Nanofluid concentration $\left(mol/m^3\right)$

α : Thermal diffusivity $\left(m^2/s\right)$

ν : Kinematic viscosity $\left(m^2/s\right)$

σ : Stefan-Boltzmann constant

ρ_f : Density of the fluid

ρ_p : Density of nano particle material

λ : Velocity slip parameter

δ : Thermal slip parameter

β : Concentration slip parameter

γ : Maxwell fluid parameter

κ : Thermal conductivity of the fluid

α_0 : Heat source parameter

Superscript

$'$: Differentiation w.r.t η

Subscripts

f : Fluid

w : Condition on the sheet

∞ : Ambient Conditions

1. INTRODUCTION

Researchers are interested in convective mass and heat transmission because of how important they are in many engineering and industrial applications. Different fluids are used to study how heat and matter move from one place to another. During this process, a lot of fluids change and many are made from scratch. The non-Newtonian fluids are being used more often than the other types. Maxwell [1] came up with the Maxwell fluid model, which is still used today, to describe how air is both stiff and flexible. Farooq, U., *et al*. [9] studied the effect of Maxwell fluid on the convective heat transfer caused by the exponentially stretching sheet. They discovered that the rate of heat transfer decreases as the thermophoresis parameter increases. Zhao *et al*. [2] looked at the Dufour and Soret effects on porous surfaces and in an MHD Maxwell fluid. Their results were published in Nature Communications. After seeing Stokes flows on a Maxwell fluid in a slip state, Vieru and Rauf [3] looked at how the wall moved in the fluid. In one paper, Ramesh *et al.* [4] suggested that a 3D Maxwell fluid approaches a stretched surface while being accompanied by heat radiation and suspended nanoparticles. Nadeem *et al*. [5] studied the heat transmission properties of an exponential stretching surface via the use of thermal stratification. According to Zheng *et al*. [6], the generalised Maxwell fluid was simulated by employing a continuously oscillating accelerating plate. Nonlinear heat radiation and activation energy flowing through a stretched surface, as discovered by Sajid *et al*. [7], influence the Maxwell fluid, according to their results. Madhu *et al*. [8] looked at the flow of a nanofluid across a stretched surface in the presence of thermal radiation effects using MHD and thermal radiation effects.

After Sakiadis [10] introduced the study of boundary layer flow over a solid surface that moves at a constant speed, many researchers have been interested in the boundary layer flow caused by a surface that is being stretched. Crane was the first person to study how the boundary layer flows over a surface that is being stretched. [11-13] have looked into different parts of the problem since then. Bhargava *et al*. [14] used FEM to study how a mixed convection micropolar fluid moves when it is surrounded by a linearly stretching sheet with uniform suction. Desseaux and Kelson [15] looked at the flow of a micropolar fluid bounded by a sheet that stretches in a straight line, while Bhargava *et al*. [16] looked at the same flow of a micropolar fluid over a sheet that stretches in a way that is not straight. Vajravelu [17] looked at flow and heat transfer in a viscous fluid over a nonlinearly stretching sheet without viscous dissipation. Cortell [18] then looked at flow and heat transfer on a nonlinearly stretching sheet with two different types of thermal boundary conditions on the sheet. Most of the above studies have used a "no-slip" condition. But when fluid flows in a micro-electro-mechanical system (MEMS), the no-slip condition at the solid-fluid interface is no longer true [19]. Fluid slippage at solid boundaries is seen in a number of situations, such as when a thin film of light oil is attached to the moving surfaces or when the surfaces are coated with special materials like a monolayer of hydrophobic octadecyltricholorosilane or in micro or nanochannels. Navier [20] has studied a general boundary condition that includes the possibility of fluid slippage at a solid boundary in order to explain the slip phenomenon. He has suggested that the tangential component of fluid velocity at the boundary walls is proportional to the tangential stress. After Navier, many authors [21-23] added to what he had done.

All the above studies did not go deep into the chemical reaction effects with heat sources, which will be useful in slip flows and convective heat and mass transfer. So in this paper we want to present the study of Maxwell-Nanofluid flow, heat and mass transfer past a stretching sheet with Multiple Slip and Chemical Reaction Effects using FEM.

2. FLOW GOVERNING EQUATIONS

The present work analyzes the combined effects of a magnetic field and cross diffusion on magneto-hydrodynamic, incompressible, viscous, and electrically conducting boundary-layer Maxwell-nano-fluid flow towards a stretched sheet that is non-linear in the presence

©2006-2023 Asian Research Publishing Network (ARPN). All rights reserved.

of an external magnetic field. We are basing our investigation on the following presumptions:

a) This fluid flow is two-dimensional, electrically conducting, viscous and incompressible.
b) It is assumed as; the plate with constant surface temperature T_w is placed in a moderate fluid of constant ambient temperature T_∞.
c) Generally, $B(x)$a variable magnetic field will be provided to the surface of the sheet while the magnetic field induced is minimal and may be justified for MHD flow at the small magnetic Reynolds number.
d) The nano-particle concentration and surface concentration φ_w, C_w are higher than the ambient value φ_∞, C_∞ respectively.

The following dimensional form of equations, under boundary-layer approximations and assumptions, governs the fluid stream of Maxwell-Nano fluid particles.
Continuity Equation:

$$\frac{\partial u}{\partial x}+\frac{\partial u}{\partial y}=0 \tag{1}$$

Momentum Equation:

$$u\left(\frac{\partial u}{\partial x}\right)+v\left(\frac{\partial u}{\partial y}\right)=\nu\left(1+\frac{1}{\beta}\right)\left(\frac{\partial^2 u}{\partial y^2}\right)-\left(\frac{\sigma B_o^2}{\rho_f}\right)u-k_o\left(u^2\frac{\partial^2 u}{\partial x^2}+v^2\frac{\partial^2 u}{\partial y^2}+2xy\frac{\partial^2 u}{\partial x\partial y}\right) \tag{2}$$

Equation of thermal energy:

$$u\left(\frac{\partial T}{\partial x}\right)+v\left(\frac{\partial T}{\partial y}\right)=\alpha\left(\frac{\partial^2 T}{\partial y^2}\right)+\tau\left\{D_B\left(\frac{\partial \varphi}{\partial y}\right)\left(\frac{\partial T}{\partial y}\right)+\frac{D_T}{T_\infty}\left(\frac{\partial T}{\partial y}\right)^2\right\}+D_{TC}\left(\frac{\partial^2 C}{\partial y^2}\right)+\frac{Q}{\rho C_P}(T-T_\infty)=0 \tag{3}$$

Equation of species concentration:

$$u\left(\frac{\partial C}{\partial x}\right)+v\left(\frac{\partial C}{\partial y}\right)=D_S\left(\frac{\partial^2 C}{\partial y^2}\right)+D_{CT}\left(\frac{\partial^2 T}{\partial y^2}\right)-k(C-C_\infty)=0 \tag{4}$$

Equation of nano particle concentration:

$$u\left(\frac{\partial \varphi}{\partial x}\right)+v\left(\frac{\partial \varphi}{\partial y}\right)=D_B\left(\frac{\partial^2 \varphi}{\partial y^2}\right)+\frac{D_T}{T_\infty}\left(\frac{\partial^2 T}{\partial y^2}\right) \tag{5}$$

For Maxwell-nano fluid flow, the boundary conditions are

$$\left.\begin{array}{l} u=u_w=ax+L_1\left(\frac{\partial u}{\partial y}\right),\ v=0,\ T=T_w+L_2\left(\frac{\partial T}{\partial y}\right),\ C=C_w+L_3\left(\frac{\partial C}{\partial y}\right),\ \varphi=\varphi_w\ \ at\ \ y=0 \\ u\to 0,\ T\to T_\infty,\ C\to C_\infty,\ \varphi\to\varphi_\infty\ \ as\ \ y\to\infty \end{array}\right\} \tag{6}$$

The following similarity variables are introduced for solving governing equations (2)-(5) as

$$\left.\begin{array}{l} \eta=y\sqrt{\frac{a}{\nu}},\ \psi=\left(\sqrt{av}\right)f(\eta),\ \theta=\frac{T-T_\infty}{T_w-T_\infty},\ S=\frac{C-C_\infty}{C_w-C_\infty},\ \phi=\frac{\varphi-\varphi_\infty}{\varphi_w-\varphi_\infty} \end{array}\right\} \tag{7}$$

Using Eq. (7), the fundamental equations (2) to (5) become

$$f'''+ff''-f'^2-Mf'-\gamma\left(f^2f''-2fff''\right)=0 \tag{8}$$

$$\theta''+\Pr f\theta'+\Pr Nb\theta'\phi'+\Pr Nt\theta'^2+DuS''+\alpha_0\theta=0 \tag{9}$$

$$S''+LefS'+Sr\theta''+SrK_0=0 \tag{10}$$

$$Nb\phi''+NbLnf\phi'+Nt\theta''=0 \tag{11}$$

And the corresponding boundary conditions (6) become

$$\left.\begin{array}{l} f=0,\ f'=1+\lambda f''(0),\ \theta=1+\delta\theta'(0),\ S=1+\beta\phi'(0),\ \phi=1\ \ at\ \ \eta=0 \\ f'\to 0,\ \theta\to 0,\ S\to 0,\ \phi\to 0\ \ as\ \ \eta\to\infty \end{array}\right\} \tag{12}$$

Where the elaborated physical parameters are defined as

$$\left.\begin{array}{l} \Pr=\frac{\nu}{\alpha},\ M=\frac{\sigma B_o^2 x}{\rho_f a},\ Le=\frac{\alpha}{D_S},\ Nb=\frac{(\rho C)_f D_B(\varphi_w-\varphi_\infty)}{(\rho C)_p \nu},\ Ln=\frac{\nu}{D_B}, \\ \beta=L_3\sqrt{\frac{a}{\nu}},\ Nt=\frac{(\rho C)_f D_T(T_w-T_\infty)}{(\rho C)_p T_\infty},\ Du=\frac{D_{TC}(C_w-C_\infty)}{\alpha(T_w-T_\infty)},\ \delta=L_2\sqrt{\frac{a}{\nu}}, \\ Sr=\frac{D_{CT}(T_w-T_\infty)}{D_S(C_w-C_\infty)},\ \gamma=k_o a,\ \lambda=L_1\sqrt{\frac{a}{\nu}},\alpha_0=\frac{Q}{a(\rho C_p)},K_0=\frac{K}{a} \end{array}\right\} \tag{13}$$

©2006-2023 Asian Research Publishing Network (ARPN). All rights reserved.

The parameters of engineering interest in heat and mass transport problems are the Skin-friction coefficient $\left(Cf\right)$, local Nusselt Number $\left(Nu_x\right)$, the Sherwood number $\left(Sh_x\right)$ and the nano-fluid Sherwood Number $\left(Sh_{x,n}\right)$. These parameters characterise the skin-friction coefficient, wall heat, the regular and nano mass transfer rates, respectively, and are defined by

$$Cf = \frac{\tau_w}{\rho_f U^2} \Rightarrow \mathrm{Re}_x^{-\frac{1}{2}} Cf = \left(1+\gamma\right) f''\left(0\right) \quad (14)$$

$$Nur = \frac{Nu_x}{\sqrt{\mathrm{Re}_x}} = \left[-\left(\frac{x}{T_w - T_\infty}\right)\left(\frac{\partial T}{\partial y}\right)\right]_{y=0} = -\left(\sqrt{\mathrm{Re}_x}\right)\theta'(0) \quad (15)$$

$$Shr = \frac{Sh_{x,n}}{\sqrt{\mathrm{Re}_x}} = \left[-\left(\frac{x}{C_w - C_\infty}\right)\left(\frac{\partial C}{\partial y}\right)\right]_{y=0} = -\left(\sqrt{\mathrm{Re}_x}\right)S'(0) \quad (16)$$

$$Sh = \frac{Sh_x}{\sqrt{\mathrm{Re}_x}} = \left[-\left(\frac{x}{\varphi_w - \varphi_\infty}\right)\left(\frac{\partial \varphi}{\partial y}\right)\right]_{y=0} = -\left(\sqrt{\mathrm{Re}_x}\right)\phi'(0) \quad (17)$$

Where $\mathrm{Re}_x = \frac{Ux}{\nu}$ be the local Reynolds number.

3. NUMERICAL SOLUTION

The differential equations (8), (9), (10), (11) are non-linear and solved these nonlinear equations subject the boundary conditions (12). Using the finite element method, the method is as follows:

- All the nonlinear ODE, are descritized along η.
- The element wise descritized equations are combined using continuity conditions.
- After integrating the residuals as given in Galerkin finite element method, the nodal values of all governing variables are obtained.
- The algebraic system is solved numerically using iterative process and the results are shown in graphical form.

For checking of program code validation, the present reduced Nusselt Number results are compared with the published results of Khan and Pop [24] in Table.1 at $\gamma = \beta = \lambda = \delta = 0$ there is a good agreement between the two sets of results

4. RESULTS AND DISCUSSIONS

The computational work is carried out with help of Mathematica 10.4 package. η is approximated to 3 for computational purpose. All the profiles of governing variables, f', θ, S, φ are drawn for variations of the non-dimensional parameters. The detailed study is as follows:

Figure-1 depicts the profile of f' with magnetic parameter M. Increase in M is reducing the magnitude of f'. It indicates that the electromagnetic force should be much more to dominate the inertial force. This is perhaps due to the presence of nano particles. Figure-2 describes the variation of f' for γ, the Maxwell parameter. The Maxwell parameter is reducing the flow field. So it is most useful in controlling the flow and helps in effective heat and mass transfer. Figure-3 gives the variation of flow with λ, the velocity slip parameter. As the slip increases the flow decreases. It is one of the aspects to control the flow field which in turn affects the heat and mass transfer.

Figure-4 shows the profile of the temperature (θ) with the magnetic parameter M. The magnetic field retards the flow and enhances the temperature. The significant effect of presence of magnetic field is observed in this profile. Figure-5 shows the variation of temperature (θ) with Maxwell parameter (γ). Temperature enhances with the Maxwell parameter (γ), it pronounces the importance of Maxwell Nano-fluid, and so all heating systems may use this fluid for efficient heating. Figure-6 describes the variation of temperature with velocity slip parameter (λ). It clears that the velocity slip retards the flow and enhances the temperature which helps the heating systems. Figure-7 represents the temperature profile with variation of diffusion slip (β). Nano-particles raise temperatures because their presence increases diffusion slip. Figure-8 shows that as thermal slip is improved, temperatures drop. So, thermal slip can be used to regulate the thermal boundary layer. Figure-9 demonstrates that when the Brownian motion parameter increases, so does the thickness of the thermal boundary layer (Nb). The results demonstrate a linear relationship between particle concentration and thermal boundary layer thickness. The gradual increase in the thermal boundary thickness has observed with increase in thermophoresis parameter (Nt), its displayed in Figure-10. Figure-11 shows the profile of temperature with heat source parameter (α). As the nano particle carries the heat temperature enhances with increase in heat source parameter near the base of the plate more. Figure-12 evidences the decrease of thermal boundary layer with increase in Sr. This implies the supremacy of diffusion over thermal boundaries. The temperature distribution for exothermic processes (K>0) is shown in Figure-13. Generative reaction affects the temperature slightly whereas the destructive chemical reaction is significantly varying the temperature. The profile describe that the presence of nano particle retards the temperature in both chemical reactions.

The diffusion profiles are displayed and the detailed study is given below. Figure-14 displays the effect of the diffusion slip (β) on diffusion. The slip is effective on diffusion and is directly proportional. This slip phenomenon can be used to enhance the bulk flow. Figure-15 shows the variation of diffusion with γ. It is found that the thermal slip and the diffusion are inversely proportional. Figure-16 shows the effect of chemical reaction on diffusion. As the reaction rate increases the bulk flow increases gradually. The chemical reaction is significant of in convective heat and mass transfer, even to control the diffusion. Figure-17 depicts the diffusion profile with variation of velocity slip parameter (λ). The

©2006-2023 Asian Research Publishing Network (ARPN). All rights reserved.

increase in slip enhances the bulk flow. The bulk flow enhancement is the main cause of temperature enhancement. Figure-18 displays the variation of diffusion with Lewis number (Le). The increase in Lewis number enhances significantly the bulk flow near the base of the plate. Figure-19 depicts the variation of diffusion with magnetic parameter M. Increase in M enhances the bulk flow, so that the Lorentz force is effective on the bulk flow. Fig. 20 shows the effect of Brownian motion parameter (Nb) on the diffusion. It is evident that the Brownian motion retards the bulk flow and proves the domination of metal particle on diffusion. Figure-21 describes the effect of thermophoresis parameter (Nt) on diffusion. Nt retards the bulk flow, it may be due to the metal particle. Figure-22 shows the variation of diffusion with Sorret number (Sr). As Sr increases the diffusion decreases showing the significance of bulk flow. Figure-23 shows the variation of diffusion with heat source parameter (α). As the heat source increases the diffusion decreases. This may be due to the presence of metal particles in the fluid. Figure-24 shows the variation of diffusion with Du. Bulk flow enhances with Du significantly showing that the solutal diffusivity dominates the thermal diffusivity.

Table-1. Comparison of results for the diminished Nusselt Number at $\gamma = \beta = \lambda = \delta = 0$.

Nb	Nt	Khan and Pop [24] results	Present Results
0.1	0.1	0.9524	0.9529117836670803
	0.2	0.6932	0.6625738216469769
	0.3	0.5201	0.539110321502154
	0.4	0.4026	0.428672071597206
	0.5	0.3211	0.3299852651475219
0.2	0.1	0.5056	0.4993154830254870
	0.2	0.3654	0.3798254203156219
	0.3	0.2731	0.2790215481302157
	0.4	0.2110	0.23932302154862313
	0.5	0.1681	0.1530215415482125

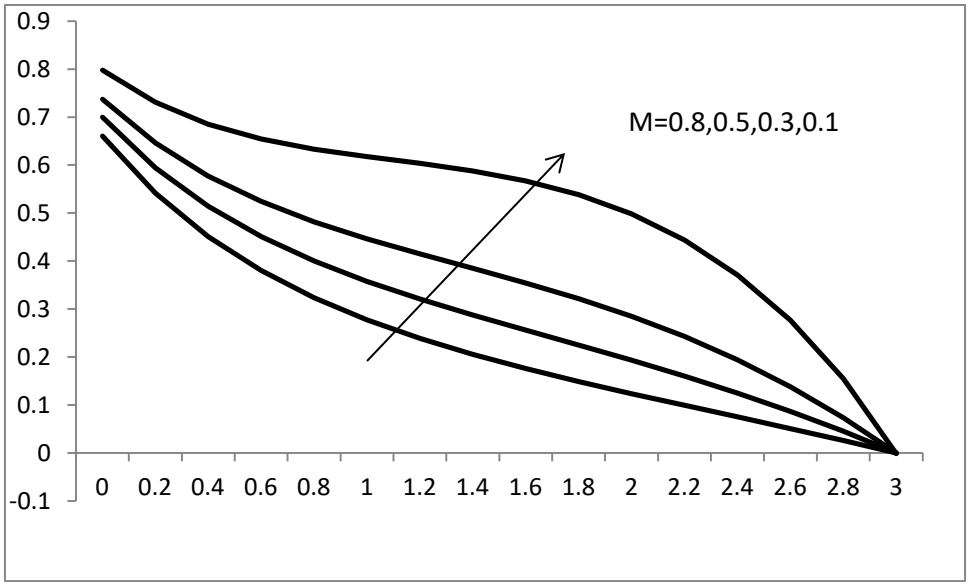

Figure-1. Variation of f' with M.

©2006-2023 Asian Research Publishing Network (ARPN). All rights reserved.

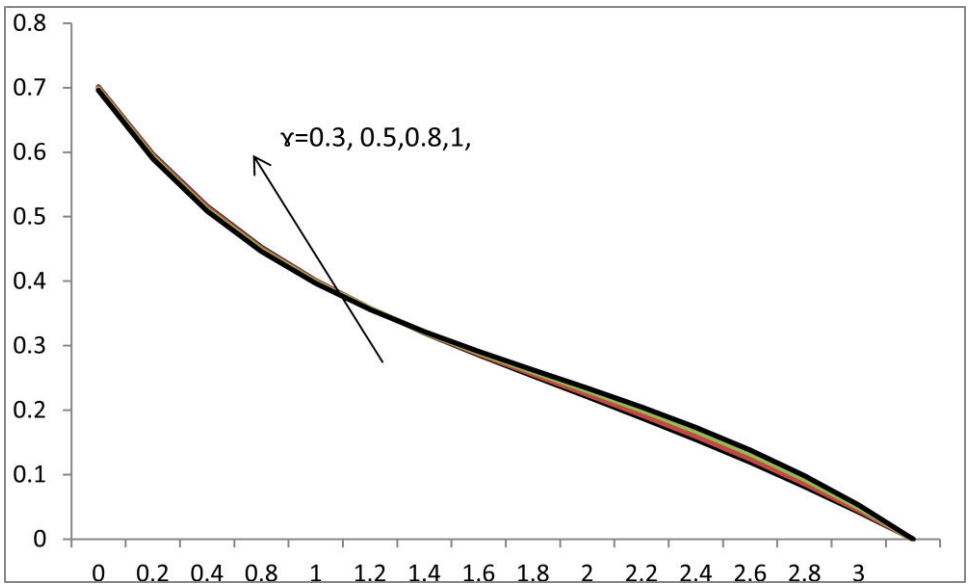

Figure-2. Variation of f' with γ.

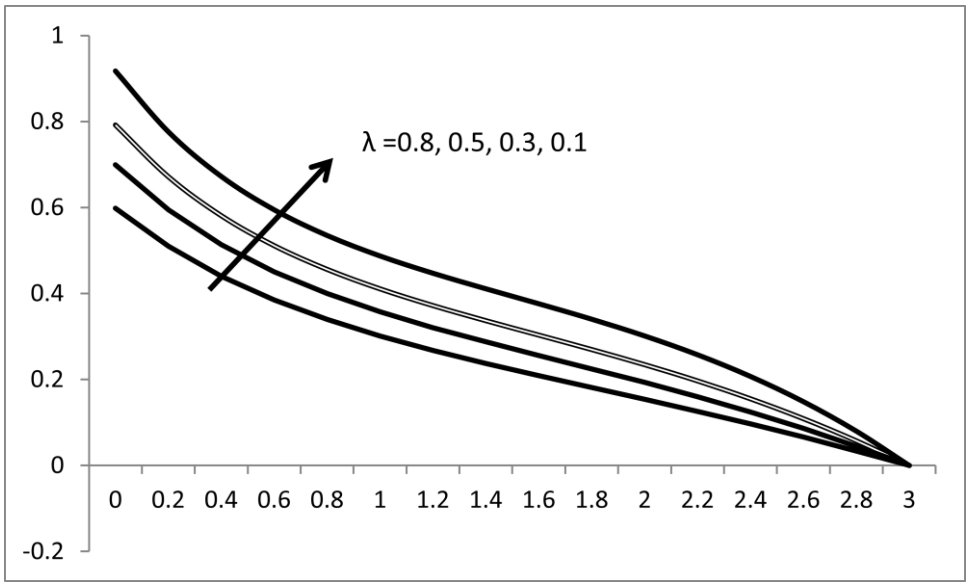

Figure-3. Variation of f' with λ.

©2006-2023 Asian Research Publishing Network (ARPN). All rights reserved.

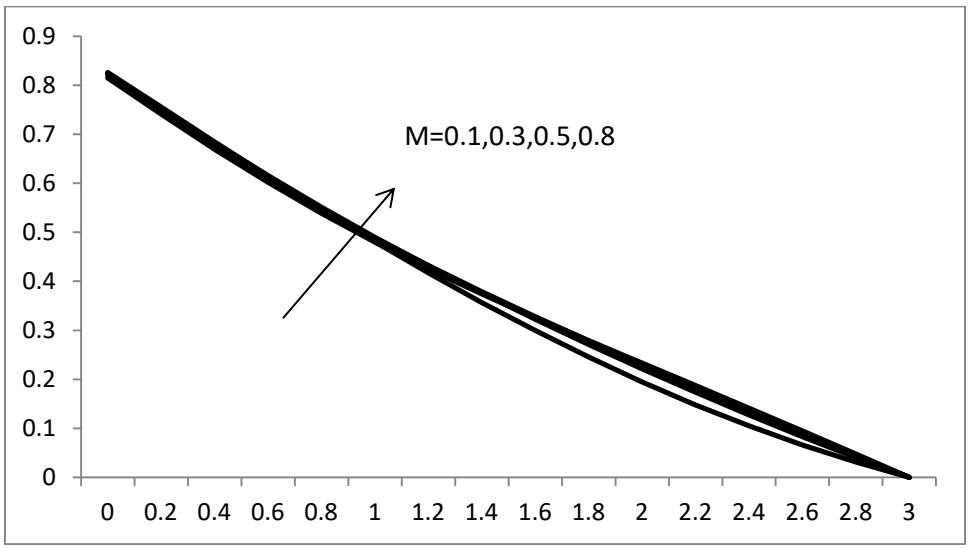

Figure-4. Variation of θ with M.

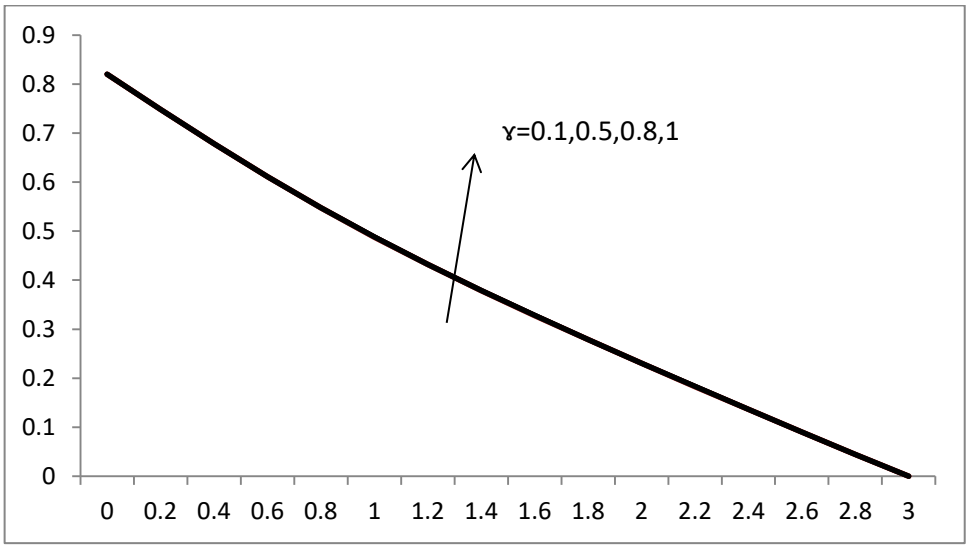

.

Figure-5. Variation of θ with γ.

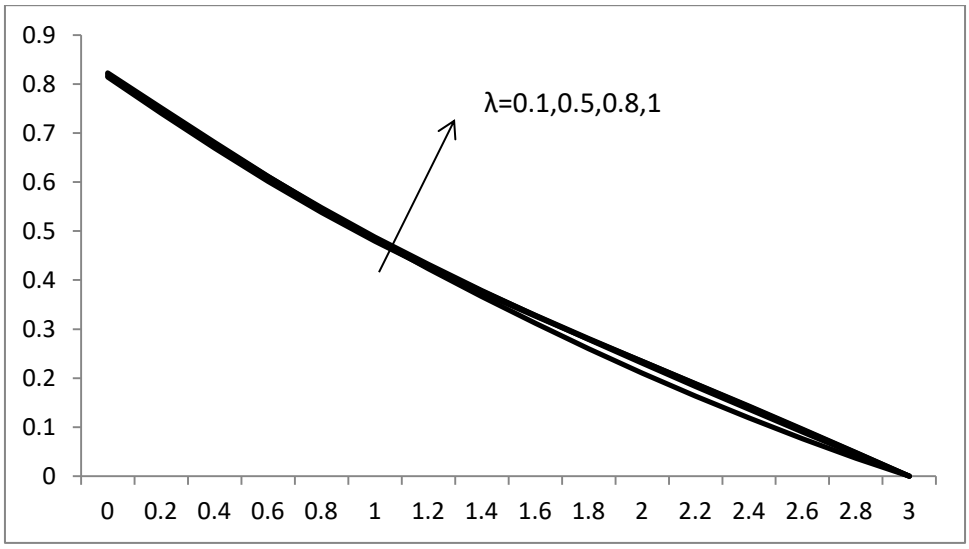

Figure-6. Variation of θ with λ.

©2006-2023 Asian Research Publishing Network (ARPN). All rights reserved.

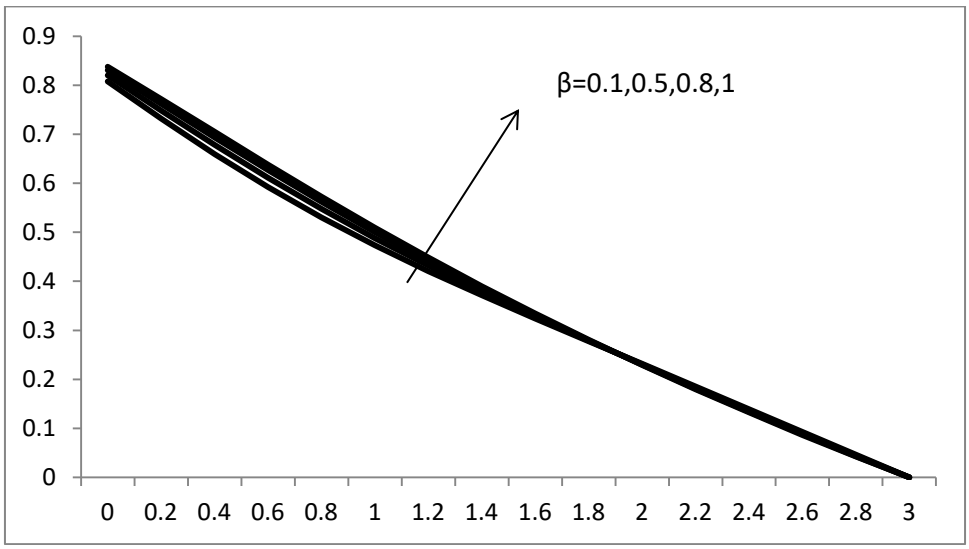

Figure-7. Variation of θ with β.

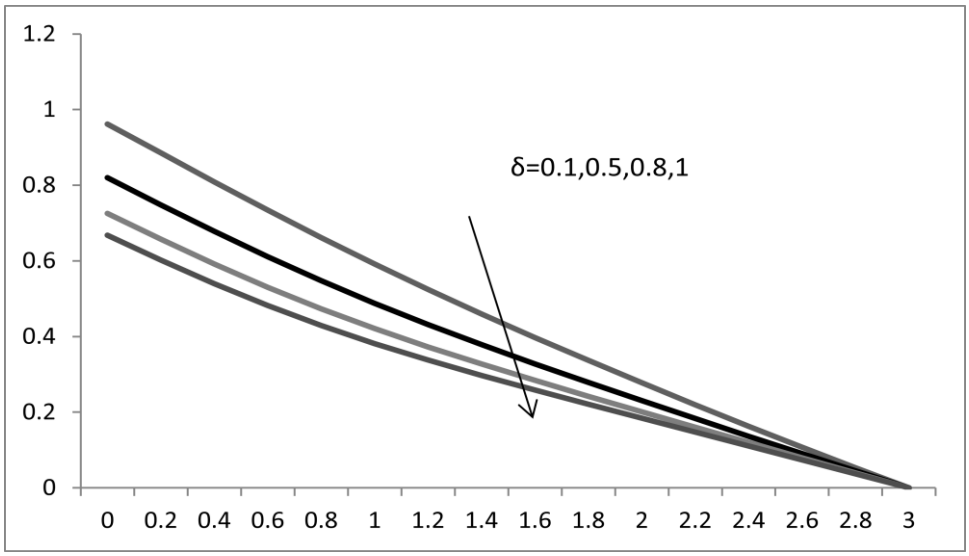

Figure-8. Variation of θ with δ.

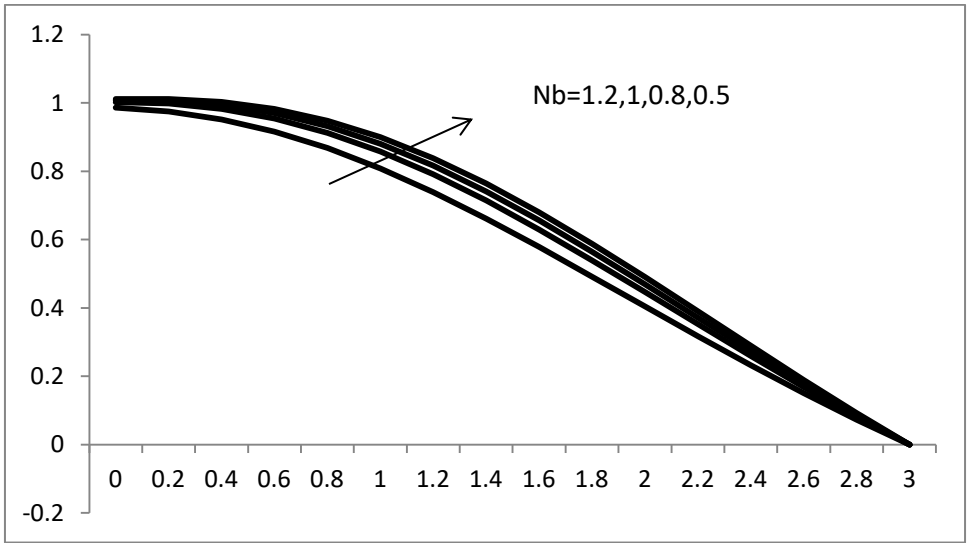

Figure-9. Variation of θ with Nb.

©2006-2023 Asian Research Publishing Network (ARPN). All rights reserved.

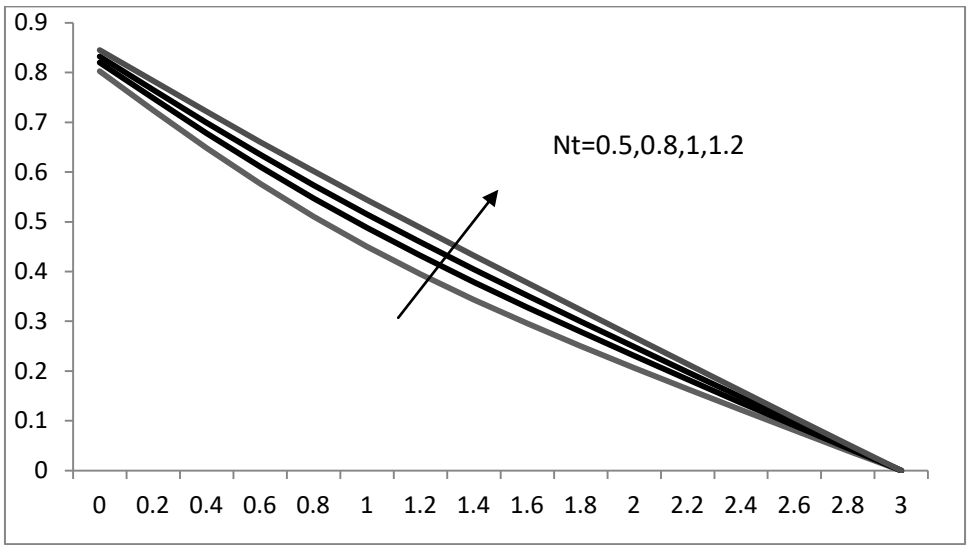

Figure-10. Variation of θ with Nt.

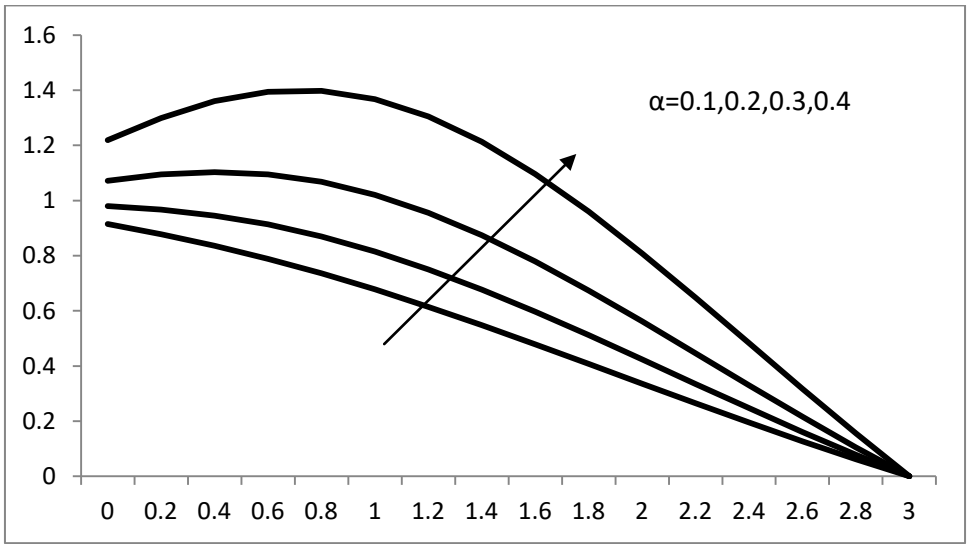

Figure-11. Variation of θ with α.

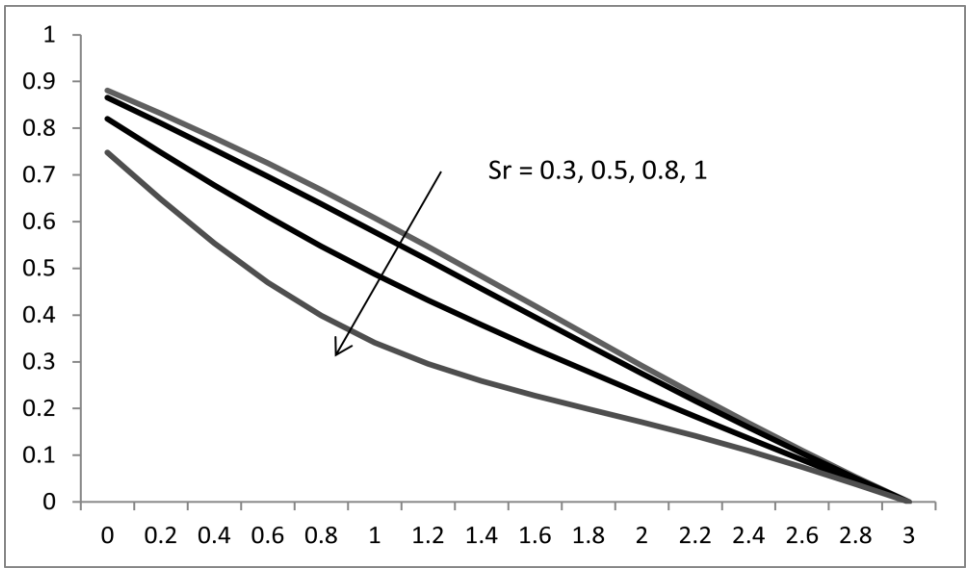

Figure-12. Variation of θ with Sr.

©2006-2023 Asian Research Publishing Network (ARPN). All rights reserved.

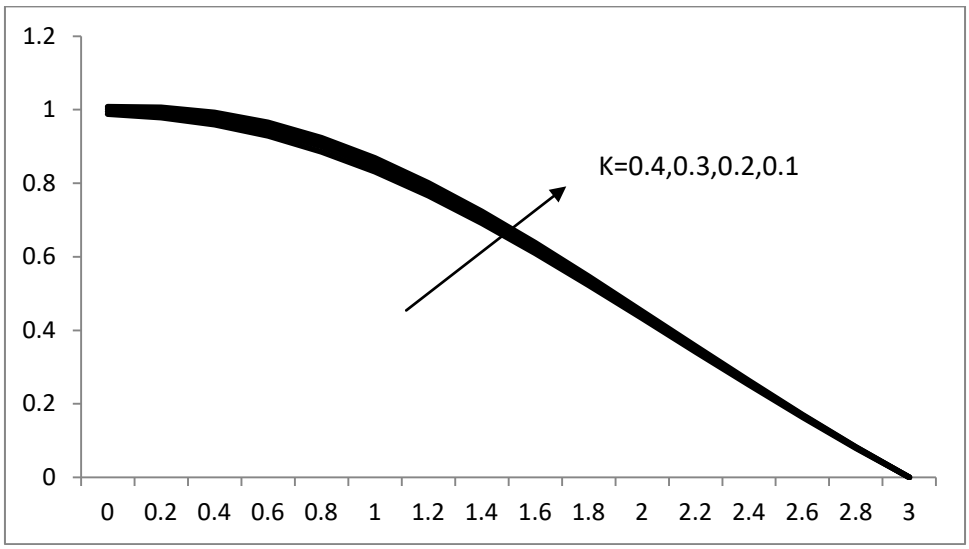

Figure-13. Variation of θ with K.

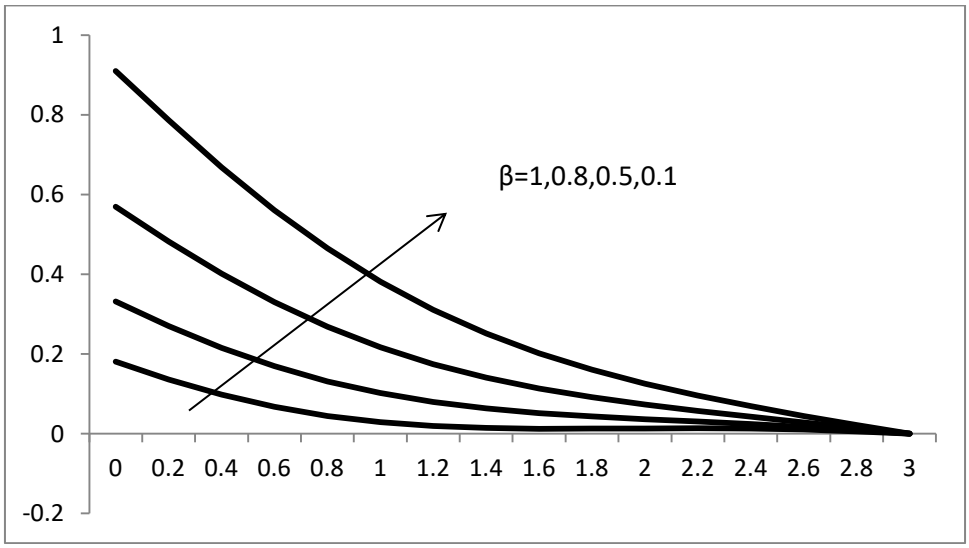

Figure-14. Variation of S with β.

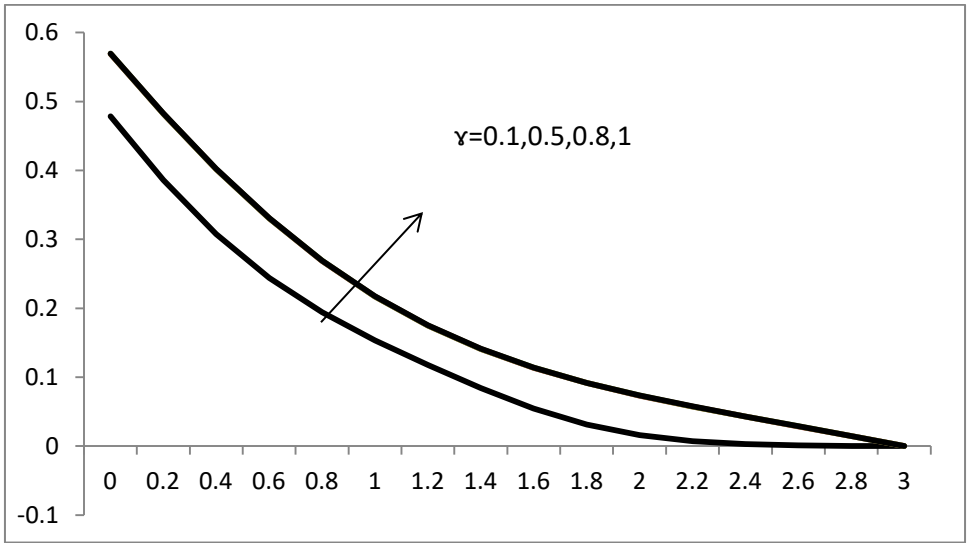

Figure-15. Variation of S with ɤ.

©2006-2023 Asian Research Publishing Network (ARPN). All rights reserved.

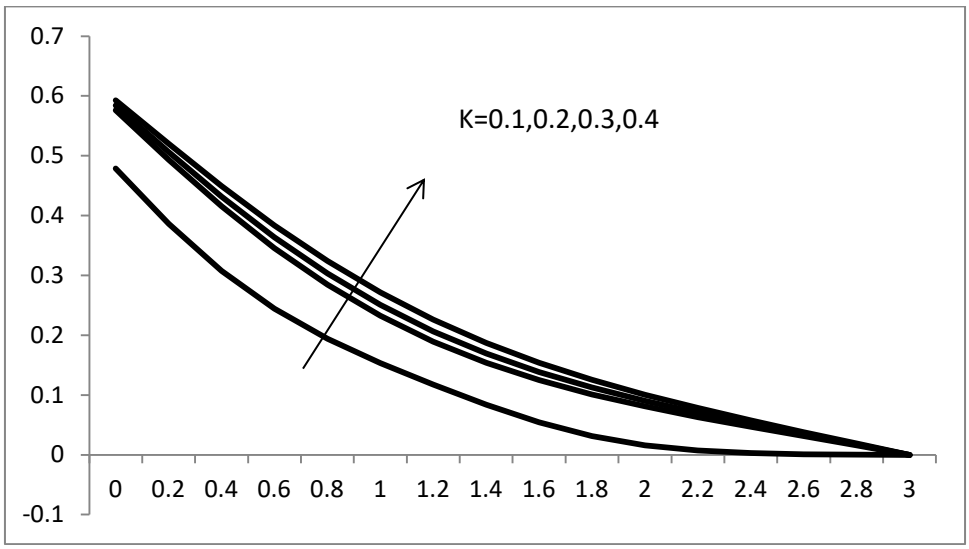

Figure-16. Variation of S with K.

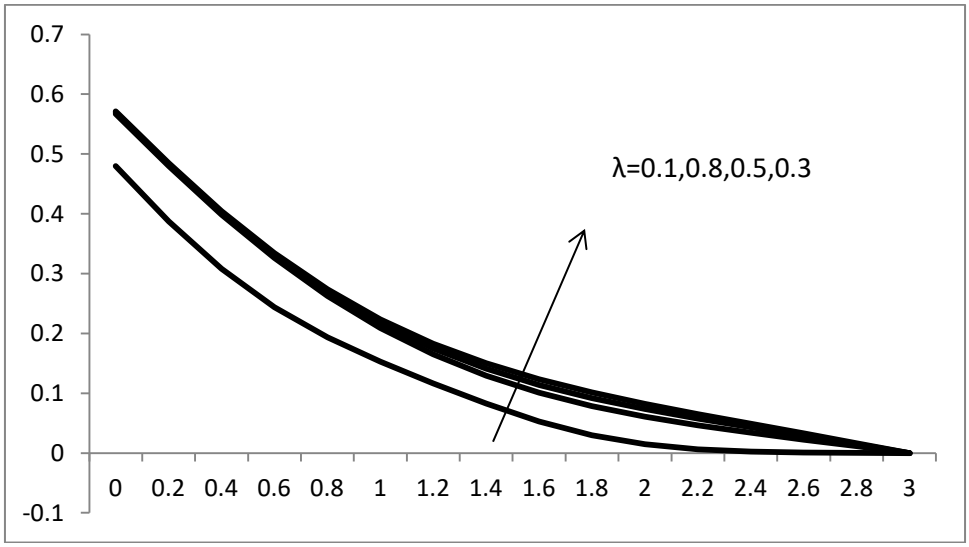

Figure-17. Variation of S with λ.

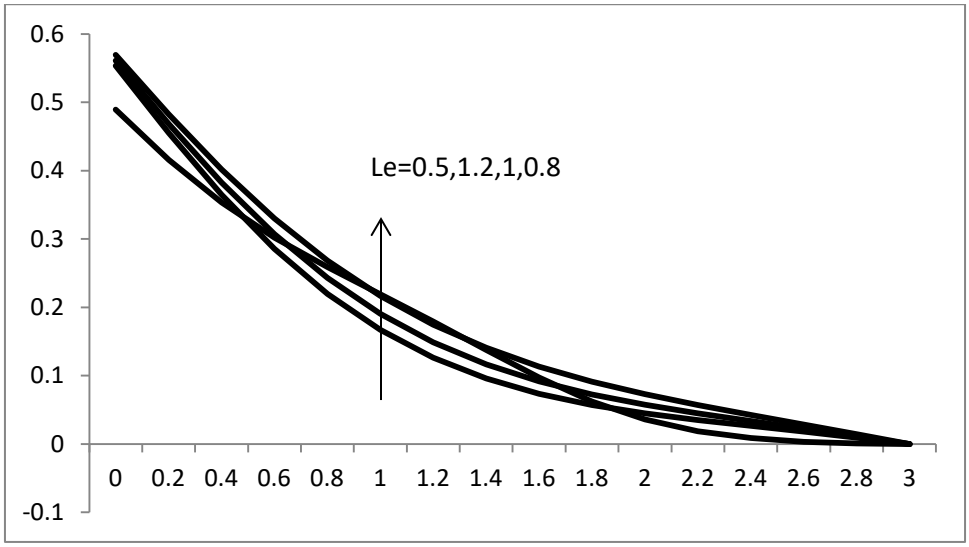

Figure-18. Variation of S with Le.

©2006-2023 Asian Research Publishing Network (ARPN). All rights reserved.

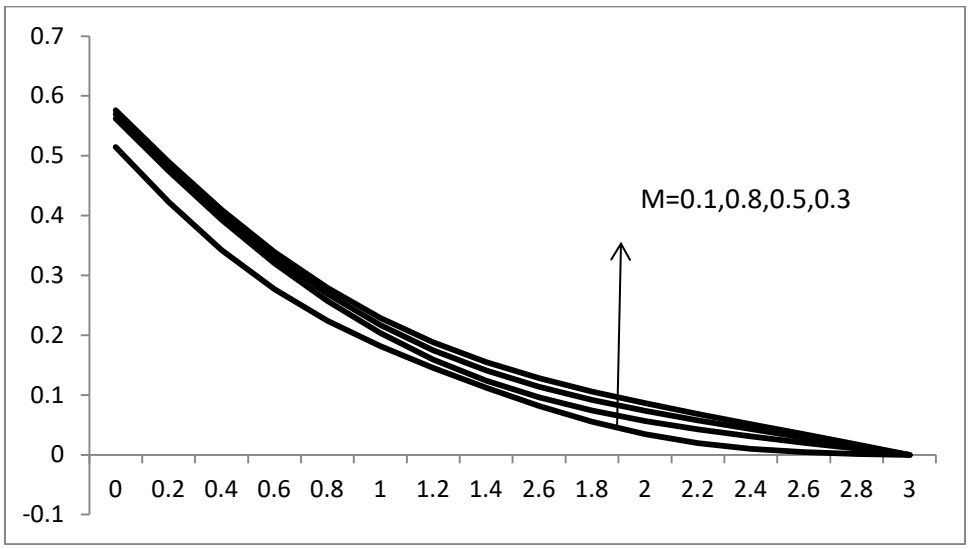

Figure-19. Variation of S with M.

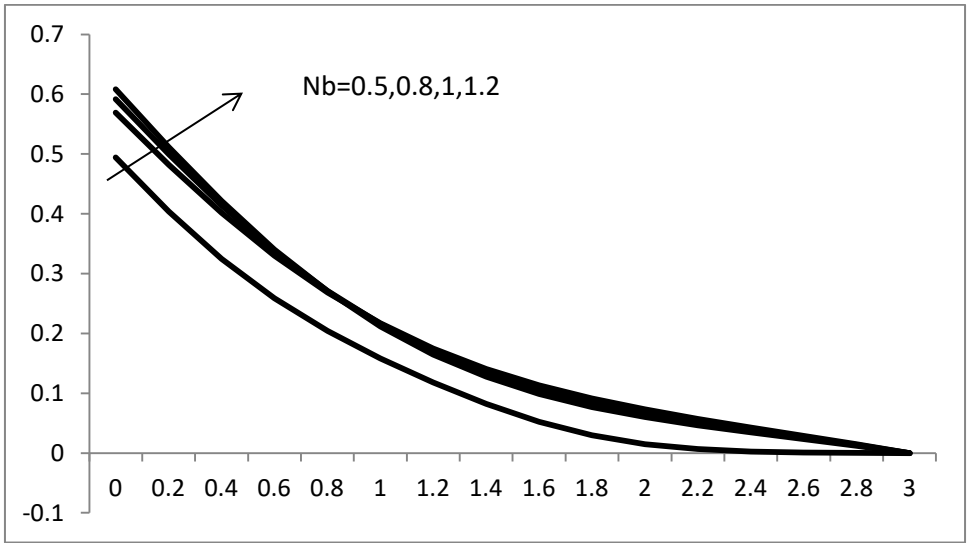

Figure-20. Variation of S with Nb.

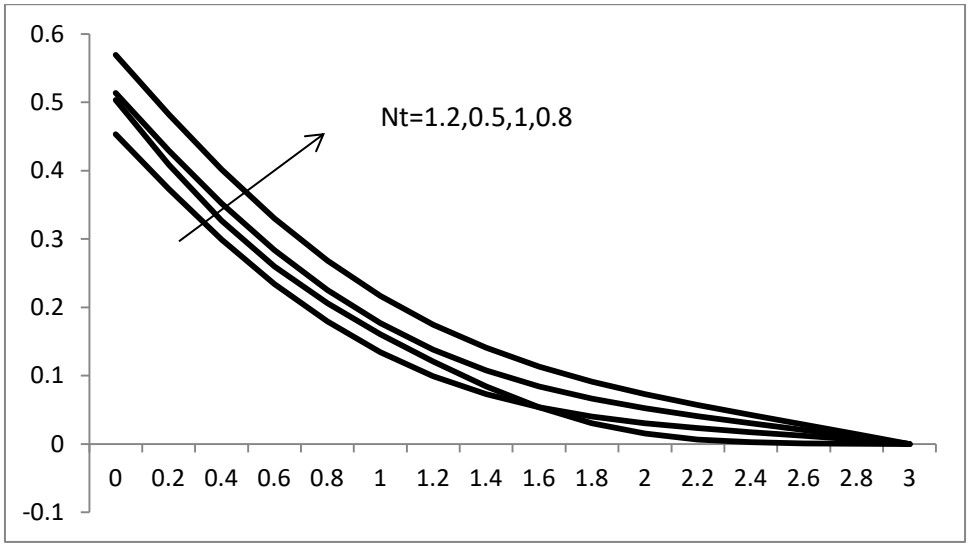

Figure-21. Variation of S with Nt.

©2006-2023 Asian Research Publishing Network (ARPN). All rights reserved.

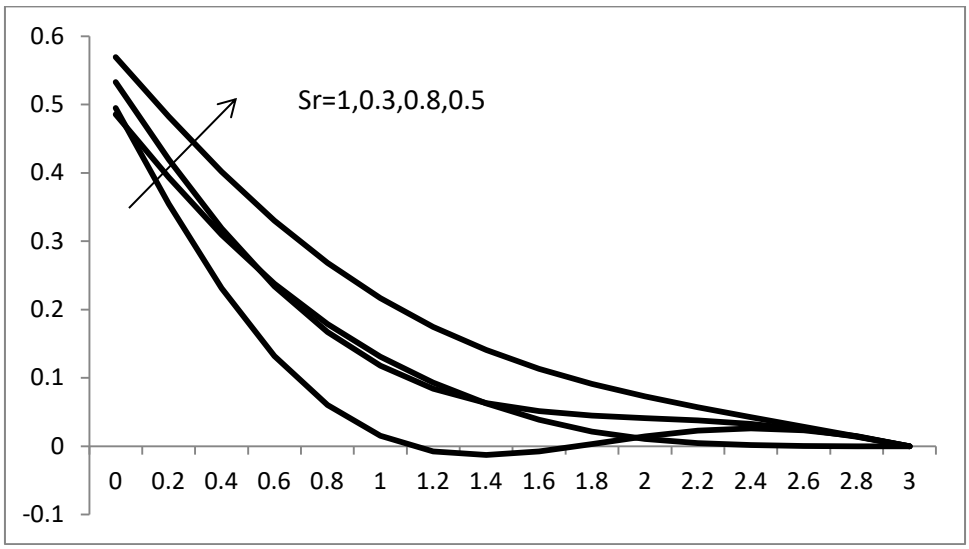

Figure-22. Variation of S with Sr.

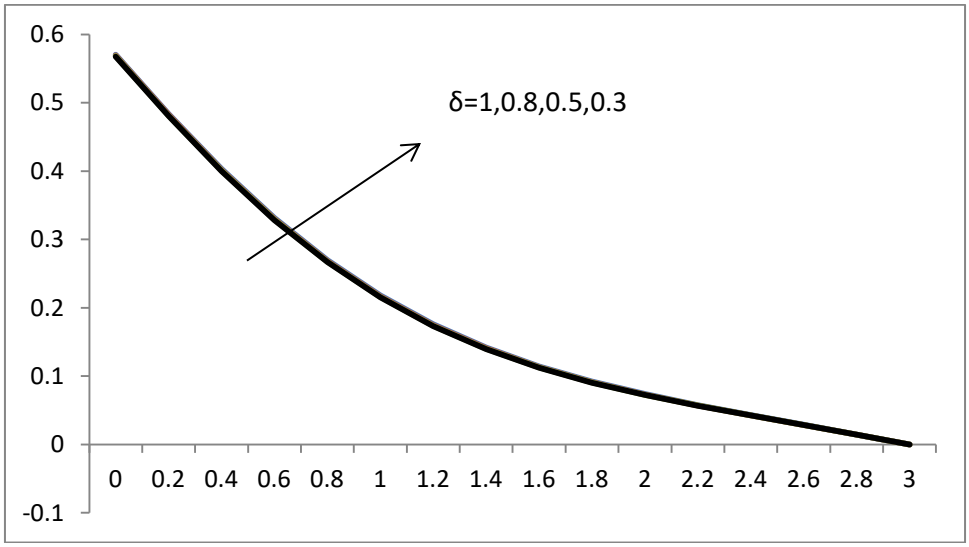

Figure-23. Variation of S with δ.

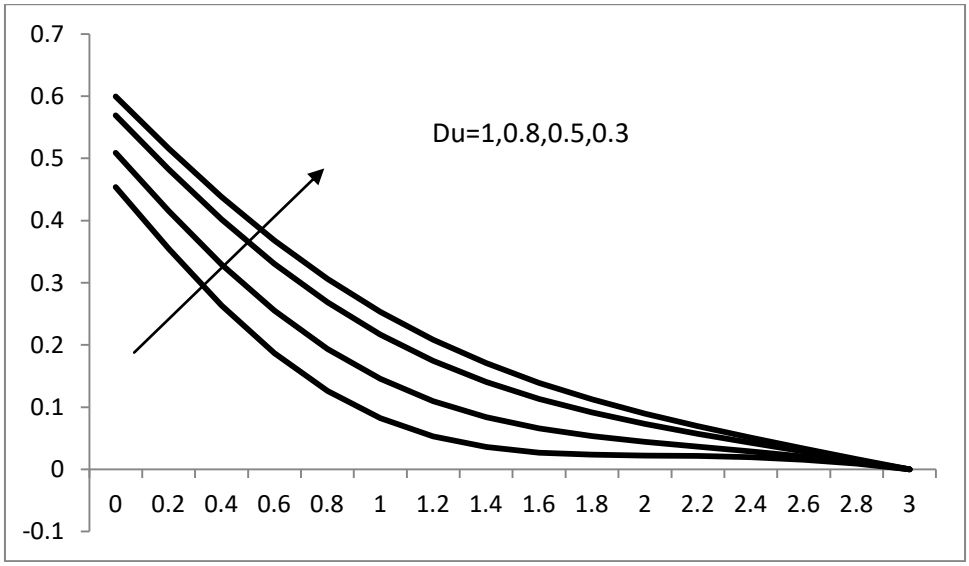

Figure-24. Variation of S with Du.

©2006-2023 Asian Research Publishing Network (ARPN). All rights reserved.

Table-2. Variation of Skin Friction (C_f).

M	γ	δ	β	Nb	Nt	λ	K	C_f
0.5	0.5	0.5	0.5	0.8	0.8	0.5	0.1	0.9010215987150805
0.1								0.5896571808634553
0.3								0.7878414253021541
0.8								1.0198663590840216
	0.1							0.9010215986959373
	0.8							0.9010215987298243
	1.0							0.9010215987398531
		0.1						0.9010215986959373
		0.8						0.9010215987298243
		1.0						0.9010215987398531
			0.1					0.5896571847350789
			0.8					0.7878414248678994
			1.0					1.0198663610317926
				0.5				0.9010215991368926
				1.0				0.9010215985513288
				1.2				0.901021598652341
					0.5			0.9010216010918037
					1.0			0.901021599580316
					1.2			0.9010216006109417
						0.1		1.2358900603008647
						0.3		1.040148251779392
						0.8		0.7532945556429594
							0.2	0.9010215985548549
							0.3	0.901021598381113
							0.4	0.9010215981911538

Table-2 displays the skin friction coefficient. Lorentz force is significant on skin friction, velocity slip retards the coefficient of skin friction but the Maxwell parameter, Chemical reaction parameter is not much significant on skin friction.

©2006-2023 Asian Research Publishing Network (ARPN). All rights reserved.

Table-3. Variation of Nusselt Number (Nur).

γ	δ	β	Nb	Nt	Du	Sr	Le	λ	K	α	Nur
0.5	0.5	0.5	0.8	0.8	0.5	0.5	0.8	0.5	0.1	0.2	0.016501153587134547
0.1											0.29337956347350236
0.8											0.016594601096655767
1.0											0.01667493964864668
	0.1										0.016249222945787532
	0.8										0.016700216432401885
	1.0										0.016838084686909158
		0.1									0.04781466152723828
		0.8									0.0053397029282138755
		1.0									0.019186199359748708
			0.5								0.028043340020315805
			1.0								0.040820668020895005
			1.2								0.06174737352827103
				0.5							0.012035041972173663
				1.0							0.03393456091751343
				1.2							0.04998223799709678
					0.3						0.03715810116496923
					0.8						0.12406467905454673
					1.0						0.22272758557073236
						0.3					0.014214250269195728
						0.8					0.08390537014265291
						1.0					0.1539433719662305
							0.5				0.007391385035299024
							1.0				0.03130307743084275
							1.2				0.045175364047692554
								0.1			0.03544298918869501
								0.3			0.005573360671353979
								0.8			0.040606778187736975
									0.2		0.004176329001159166
									0.3		0.009368361760216767
									0.4		0.024387988106218495
										0.1	0.10730599387949688
										0.3	0.18488201630995557
										0.4	0.4346673020969356

Nusselt Number values are depicted in Table-3. Maxwell parameter reduces the rate of heat transfer particularly for smaller values of γ, which is useful in cooling systems. Thermal slip enhances the rate of heat transfer slightly. Nb and Nt enhances the heat transfer rate near the base of the plate. Du and Sr enhances the heat transfer rate significantly. It is observed that the chemical reaction and heat source are enhancing the rate of heat transfer effectively.

©2006-2023 Asian Research Publishing Network (ARPN). All rights reserved.

Table-4. Variation of Sherwood Number (Shr).

M	γ	δ	β	Nb	Nt	Du	Sr	Le	Ln	λ	K	α	Shr
0.5	0.5	0.5	0.5	0.8	0.8	0.5	0.5	0.8	0.8	0.5	0.1	0.2	0.8616925547334483
0.1													0.8317127248095397
0.3													0.8481896865427079
0.8													0.8760622094300662
	0.1												1.0428493129784704
	0.8												0.861054841071491
	1.0												0.860659819860321
		0.1											0.8592940349066119
		0.8											0.863547390858919
		1.0											0.864812461853163
			0.1										0.8991449496113062
			0.8										0.835590942082109
			1.0										0.8190521446083785
				0.5									0.9818486277515391
				1.0									0.8168909761961194
				1.2									0.7845568155560825
					0.5								0.7125401467046034
					1.0								0.9737112123776022
					1.2								1.0945432293576487
						0.3							0.8007158586351847
						0.8							0.9825851735437442
						1.0							1.0920389233110364
							0.3						0.8279158374386532
							0.8						0.9354376675736371
							1.0						1.0116367353706497
								0.5					0.8342863388661312
								1.0					0.8784192773385163
								1.2					0.8939500453503024
									0.5				0.8008510027091249
									1.0				0.9016072194726007
									1.2				0.9408527070218562
										0.1			0.8518529441095232
										0.3			0.8569905321564806
										0.8			0.8669973265010331
											0.2		0.8478681803338752
											0.3		0.832673388503395
											0.4		0.8158212227122463
												0.1	0.720291158055837
												0.3	1.0550578006521618
												0.4	1.3441048414158672

©2006-2023 Asian Research Publishing Network (ARPN). All rights reserved.

Sherwood Number variations are shown in Table-4 above for various non-dimensional parameters. Lorentz force enhances the mass transfer rate slightly. On the other hand, the Maxwell parameter retards the mass transfer rate and boosts the diffusivity. Diffusion slip is shown to increase the diffusion rate. Mass transfer is accelerated by Du, but slowed by Le, Ln, and K. But the heat source improves the mass transfer rate along the plate.

5. CONCLUSIONSS

Lorentz force enhances the skin friction and the mass transfer rate. So the magnetic field has significant impact on flow, heat and mass transfer. Velocity slip retards the flow, enhances the heat transfer rate. Thermal slip enhances the heat and mass transfer rate slightly. Because of its effect on skin friction, diffusion slip slows down the speed at which heat and mass are transferred. Incorporating a heat source increases the rate of heat and mass transmission. This research demonstrates the need of considering not just one but numerous slip effects, heat source, and chemical reaction.

REFERENCES

[1] J. C. Maxwell. 1876. Dynamical theory of gases, Philos. Trans. R. Soc. 157, pp. 49-88, 10.1098/rstb.1867.0004.

[2] J. Zhao, L. Zheng, X. Zhang, F. Liu. 2016. Convection heat and mass transfer of fractional MHD Maxwell fluid in a porous medium with Soret and Dufour effects, Int. J. Heat Mass Tran. 103, pp. 203-210.

[3] D. Vieru, A. Rauf. 2011. Stokes flows of a Maxwell fluid with wall slip condition, Can. J. Phys. 89(10): 1061-1071.

[4] G. K. Ramesh, B. C. Prasannakumara, B. J. Gireesha, S. A. Shehzad, F. M. Abbasi. 2017. Three-dimensional flow of Maxwell fluid with suspended nanoparticles past a bidirectional porous stretching surface with thermal radiation, Thermal Sci. Eng. Progress. 1, pp. 6-14.

[5] S. Nadeem, S. Ahmad, N. Muhammad, M. T. Mustafa. 2017. Chemically reactive species in the flow of a Maxwell fluid, Results in Physics. 7, pp. 2607-2613.

[6] L. Zheng, F. Zhao, X. Zhang. 2010. Exact solutions for generalized Maxwell fluid flow due to oscillatory and constantly accelerating plate, Nonlinear Anal. R. World Appl. 11(5): 3744-3751.

[7] T. Sajid, M. Sagheer, S. Hussain, M. Bilal. 2018. Darcy-Forchheimer flow of Maxwell nanofluid flow with nonlinear thermal radiation and activation energy, AIP Adv. 8(3): Article 035102.

[8] M. Madhu, N. Kishan, A. J. Chamkha. 2017. Unsteady flow of a Maxwell nanofluid over a stretching surface in the presence of magneto-hydromagnetic and thermal radiation effects, Propul. Power Res. 6(1): 31-40.

[9] U. Farooq, D. Lu, S. Munir, M. Ramzan, M. Suleman, S. Hussain. 2019. MHD flow of Maxwell fluid with nanomaterials due to an exponentially stretching surface, Sci. Rep. 9, p. 7312.

[10] Crane LJ. 1970. Flow past a stretching plate. Z Angrew Math Phys. 21: 645-7.

[11] Dutta B. K., Roy P. and Gupta AS, 1985. Temperature field in the flow over a stretching sheet with uniform heat flux. Int. Commun Heat Mass Trans. 12: 89-94.

[12] Chen CK, Char MI. 1988. Heat transfer of a continuous stretching surface with suction or blowing. J math Anal Appl. 135: 568-80.

[13] Kelson NA, Desseaux A. 2001. Effect of surface condition on flow of micro polar fluid driven by a porous stretching sheet. Int. J Eng Sci. 39: 1881-97.

[14] Bhargava R., Kumar L., Takhar HS. 2003. Finite element solution of mixed convection micro polar fluid driven by a porous stretching sheet. Int. J Eng Sci. 41: 2161-78.

[15] Desseaux A., Kelson NA. 2003. Flow of a micro polar fluid bounded by a stretching sheet. ANZIAM J. 42: C536-60.

[16] Bhargava R., Sharma S., Takhar HS, Beg OA, Bhargava. 2007. Numerical solution for for micropolar transport phenomena over a nonlinear stretching sheet. Nonlinear Anal: Model Cont. 12: 45-63.

[17] Vajravelu K. 2001. Viscous flow over a nonlinearly stretching sheet. Appl Math Comput. 124: 281-8.

[18] Cortell R. 2007. Viscous flow and heat transfer over a nonlinearly stretching sheet. App Math Comput. 184: 864-73.

©2006-2023 Asian Research Publishing Network (ARPN). All rights reserved.

[19] K. Das, T. Chakraborty and P. K. Kundu. 2015. Slip effects on nanofluid flow over a nonlinear permeable stretching surface with chemical reaction. Journal of Mechanical Engineering Science. 0(0): 1-10.

[20] Navier CLMH. 1823. Mmoir sur les lois du movement des fluids. Mn Acad Roy Sci Inst France. 6: 389-440.

[21] Zheng L., Niu J, Zhang X., *et al*. 2012. MHD flow and heat transfer over a porous shrinking surface with velocity slip and temperature jump. Math comput Model, 56: 133-144. 44 Gossaye A. Adem and Naikoti Kishan

[22] Das K. 2012. Impact of thermal radiation on MHD slip flow over a flat plate with variable fluid properties. Heat Mass Transfer. 48: 767-778.

[23] Zheng L., Liu N., Niu J., *et al*. 2013. Slip buoyancy lift effects on the mixed convection flow and radiation heat transfer of a micro fluid toward vertical permeable plate. J Porous Media. 16: 575-583.

[24] W. A. Khan, I. Pop. 2010. Boundary-layer flow of a nanofluid past a stretching sheet. International Journal of Heat and Mass Transfer. 53(11-12): 2477-2483.